Force-fight problem in control of aileron's plane

Ying Zhang*, Zhaohui Yuan

School of automation, Northwestern Polytechnical University, Xi'an, China

Received 1March 2014, www.tsi.lv

Abstract

In order to reduce or eliminate the force-fight phenomenon of single feedback loop of redundant-channels, modelling the whole control system on the basis of analysing the structure of aileron, the correctness of the model is verified by experiments. Simulation results show that set the dead band of the valve which control the feedback loop smaller is conducive to the decrease of system's fighting-force; for every reduce in the difference of the two valves' overlap of 0.01mm, the fighting-force decreases one time; when the driving speed is more than 50mm/s, system abstains smaller fighting-force. Therefore, the optimization of structure parameters can reduce fighting-force effectively. When the parameters of valves and driving speed is restricted, another method of using a bypass orifice to connect the two cavities of the cylinder is proposed to solve the problem, simulation results shows that fighting-force reduce 2000N for every increase in the orifice's diameter of 0.1mm when using the fixed orifice, and using the variable orifice can abstain a small fighting-force and meanwhile reduce the wastage of hydraulic oil.

Keywords: single feedback loop, force-fight phenomenon, difference of the two valves' overlap, driving speed of motor, bypass orifice

1 Introduction

Cross-linking and interference problem between channels of redundant steering gears that is multiple steering gears driving a comprehensive shaft which is used on aircrafts and space vehicles is called force-fight phenomenon [1, 2]. The redundant steering gear is the key component of a flight control system, in order to improve its reliability and security, the main control surface usually adopts parallel actuators. Due to the error accumulation during the process of manufacture and installation of valves and actuators, the displacement of each actuator is usually different, coupled with the large torsional stiffness of the control shaft there will be force-fight between the actuators which is easy to cause fatigue and failure of the structure [3-5], therefore the flight control system needs to take effective measures to reduce or eliminate this phenomenon. Boeing-777 adopts the differential pressure transducer to transmit fighting-force to the instruction set to equilibrate the force to reduce force-fight [6]. In F/A-18 the two channels share a main control valve, this kind of design can ensure the synchronism of the two actuators by controlling the precision of the spool [7]. In Su30 a throttle valve is used to connect the two cavities to reduce force-fight [8]. Usually the actuators are designed to work independently and each has a feedback channel in common control structure of rudder surface, as long as the consistency of all the actuators is controlled within a small range the fighting-force will not be very large [9-13], but for the certain control structure studied in this paper, the two parallel branches share only one feedback channel to simplify the structure, the fighting-force will be very large and it is easy to cause structural damage if one control valve is shut off but another one is still open [14-20]. On the bases of analysing the characteristics of the single feedback loop control structure, using MATLAB/SIMULINK to model and simulate the whole system precisely incorporating nonlinearities and the pressure loss of pipelines, the accuracy of the model is verified by experiments and several factors which have great influence on the force-fight are analysed. A method of adopting a bypass orifice is used to reduce the fighting-force and the selection of the orifice's diameter is analysed. To reduce oil consumption, the variable orifice is designed, simulation results show that this method can effectively reduce the fighting-force and the wastage of oil.

2 Structure and working principle

The schematic diagram of the system is shown in Figure 1. This system mainly consists of driving motor, mechanical transmission part, overlap valves, actuator cylinders, pipelines and a shaft. Driving motor is used to control the movement of the joystick. The two throttles of the overlap valve are connected to the cavities of the actuator cylinder through the pipelines. The head port of actuator is hinged-supported on the airframe and the piston rod of rod port is hinged-supported on the shaft.

During of flight the aileron deflects with the pull and push of the joystick controlled by the driving motor. When the joystick is pushed forward, the two plate valves open clockwise and the high-pressure oil flows into the left cavity of cylinder which will make the rod push the shaft rotates clockwise. This is a single feedback loop system, since the feedback channel is connected to one

* ***Corresponding author*** e-mail: zhangying_1102@163.com

end of the shaft next to the piston rod 1 so the feedback signal is decided by the torque on the shaft produced by piston rod 1 and has nothing to do with piston rod 2.

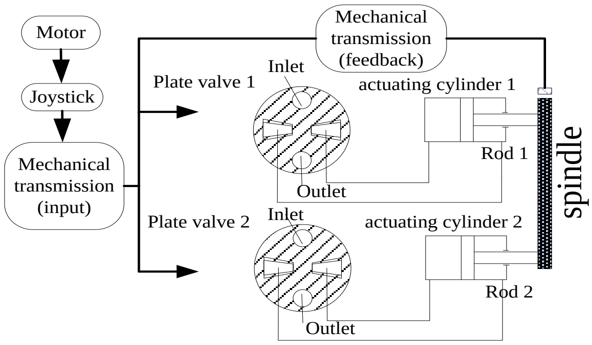

FIGURE 1 Schematic diagram

The feedback angle will make the plate valves rotate anticlockwise until both of them are closed. The difference of the two actuators' displacements will produce torsional moment on the shaft, and in turn, there will be counterforce on the two piston rods equal and opposite. The system balance will be reached until the differential pressure of cylinder's two cavities and the force on the piston rod are equal. The system's fighting-force is defined as half of the difference of the reaction force on each piston rod caused by the torsion of shaft.

3 Mathematical model

3.1 FLOW EQUATION OF PLATE VALVE

The structure of the overlap valve is shown in Figure 2.

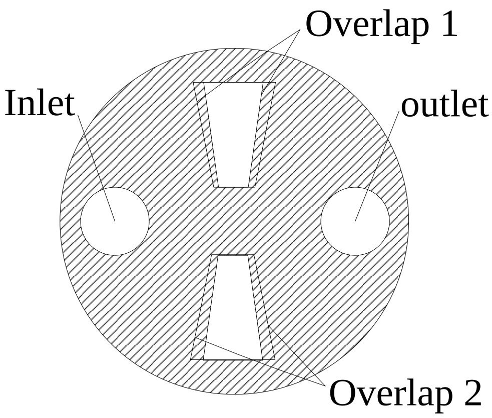

FIGURE 2 Overlap valve

The overlap valve consists of two discs, the one at bottom is show in Figure 2 which consists of an inlet and an outlet (mutual isolated) and two trapezoidal throttles, another disc covers on it which has two larger trapezoidal covers, the difference of the areas of the covers and throttles are called the overlap. The overlap of the plate valve is set to f_0, f is the open area of the throttle corresponding to the rotation of valve. The input and output flow rates of the two throttles are calculated as:

$$\begin{cases} Q_{11} = c_V(f - f_0)\sqrt{2(p_s - p_1)/\rho} & \\ Q_{12} = c_V(f - f_0)\sqrt{2(p_2 - p_0)/\rho} & (f > f_0) \\ Q_{11} = 0 & \\ Q_{12} = 0 & (f < f_0) \end{cases}, \quad (1)$$

where Q_{11},Q_{12} is the input and output flow rate of plate valve respectively, Cv is the coefficient of flow, P_1 and P_2 is the output and input pressure respectively, ρ is the density of oil, P_0 is the return pressure, P_s is the source pressure.

3.2 CONTINUITY EQUATION OF ACTUATOR

The actuator is asymmetric, so the effective area of the two cavities is not the same, the actuator works in two ways as show in Figure 3.

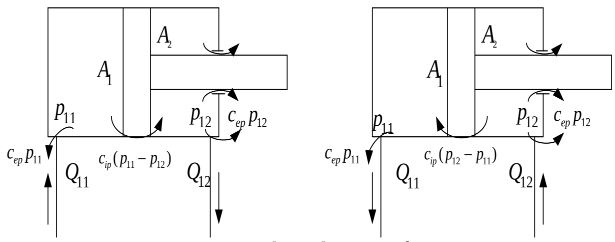

FIGURE 3 Working diagram of actuator

The continuity equation of actuator is presented as:

$$\begin{cases} Q_{11} = A_1\dfrac{dx_{t1}}{dt} + \dfrac{(x_{01}+x_{t1})A_1}{E_y}\dfrac{dp_{11}}{dt} + C_{ip}(p_{11}-p_{12}) + C_{ep}(p_{11}-p_0) \\ Q_{12} = A_2\dfrac{dx_{t1}}{dt} - \dfrac{(x_{02}-x_{t1})A_2}{E_y}\dfrac{dp_{12}}{dt} + C_{ip}(p_{11}-p_{12}) - C_{ep}(p_{12}-p_0) \end{cases}, \quad (2)$$

where P_{11} is the oil pressure of head port, P_{12} is the oil pressure of rod port, Q_{11} is the flow rate which flow into head port, Q_{12} is the flow rate which flow out from rod port. A_1 is the effective area of head port, A_2 is the effective area of rod port, x_{01} is the initial displacement of head port, x_{02} is the initial displacement of rod port, Cip and Cep are the internal and external leakage coefficient respectively, Ey is the modulus of elasticity, x_{t1} is displacement of the rod.

In the course of work the head port is hinged-supported, cause the fixed stiffness of cylinder is considered, the connection part may have certain deformation during the dynamic process which means that the cylinder body itself has certain displacement and it is set to x_c, so the rod's displacement relative to cylinder is set to (x_t-x_c), so the continuity equation is expressed as:

$$\begin{cases} Q_{11} = A_1\dfrac{d(x_{t1}-x_{c1})}{dt} + \dfrac{(x_{01}+x_{t1}-x_{c1})A_1}{E_y}\dfrac{dp_{11}}{dt} + C_{ip}(p_{11}-p_{12}) + C_{ep}(p_{11}-p_0) \\ Q_{12} = A_2\dfrac{d(x_{t1}-x_{c1})}{dt} - \dfrac{(x_{02}-(x_{t1}-x_{c1}))A_2}{E_y}\dfrac{dp_{12}}{dt} + C_{ip}(p_{11}-p_{12}) - C_{ep}(p_{12}-p_0) \end{cases}. \quad (3)$$

3.3 DYNAMIC EQUILIBRIUM EQUATION

3.3.1 Equilibrium equation of piston rod

The output force of piston rod that is the pressure differential of the two cavities should be balanced with the load, which including the inertia force of rod and load, viscous damping force, friction and elastic force which is caused by the deformation of the piston rod. The dynamic equilibrium equation of piston rod is presented as:

$$p_{11}A_1 - p_{12}A_2 = m_t \frac{d^2 x_{t1}}{dt^2} + B_t \frac{d(x_{t1} - x_{c1})}{dt} + K_{s2}x_{l1} + f_L + F_L \,, \quad (4)$$

where m_t is the equivalent mass of both piston and load, B_t is the viscous damping coefficient of piston and load, K_{S2} is the joint stiffness between piston rod and load, x_{l1} is the deformation of the piston rod, f_L is the frictional resistance of piston rod, F_L is the aerodynamic load.

3.3.2 Equilibrium equation of cylinder

The force applied to the actuator cylinder include the hydraulic pressure of the two cavities, the inertia force of the cylinder, viscous damping force and the force caused by the deformation of the hinged-supported part. The equilibrium equation of cylinder can be expressed as:

$$p_{11}A_1 - p_{12}A_2 = -m_c \frac{d^2 x_{c1}}{dt^2} - B_t \frac{d(x_{c1} - x_{t1})}{dt} - K_{s1}x_{c1} \,, \quad (5)$$

where m_c is the mass of cylinder, K_{s1} is the fixed stiffness where the cylinder is hinged-supported.

3.4 FRICTION LOSS OF PIPELINE

Considering the friction loss of the pipeline from plate valve to cylinder, the relationship of the pressure in the two cavities and the input/output pressure of the plate valve can be expressed as:

$$\begin{cases} p_{11} = p_1 - \Delta p_{11} \\ p_{12} = p_2 + \Delta p_{12} \end{cases} , \quad (6)$$

where Δp_{11} is the friction loss on the way the hydraulic oil flow into the actuator cylinder from plate valve, Δp_{12} is the friction loss on the way the hydraulic oil flow back to plate valve from cylinder.

The friction loss not only include the pressure loss when oil passes through straight pipeline but also include the pressure loss when oil passes through the bended places of pipeline, the two condition have different formulations.

The formulation of the friction loss of straight pipeline is presented as:

$$\Delta p_\lambda = \lambda \frac{l}{d} \frac{\rho v^2}{2} \,, \quad (7)$$

where Δp_λ is the friction loss, λ is the frictional resistance factor, l is the length of the pipeline, d is the diameter of the pipeline, v is the average velocity of flow in pipeline.

This formulation can be not only applied in laminar flow but also applied in turbulent flow, the value of the resistance factor λ is different in the two cases. In the process of calculation, the Reynolds number is real-time monitored to confirm the value of resistance factor λ, which can be expressed as:

$$\begin{cases} \lambda = 75/\mathrm{Re} & (\mathrm{Re} < 2320) \\ \lambda = 0.3164/\mathrm{Re}^{0.25} & (\mathrm{Re} > 2320) \end{cases} . \quad (8)$$

When the pipeline is bended the friction loss should be considered too, for circular tube the pressure loss of the bended place in pipeline is presented as:

$$\Delta p_\xi = \xi \frac{\rho v^2}{2} = \frac{7.878\rho}{\pi^2 d^4} Q^2 \,, \quad (9)$$

Where ΔP_ξ is called local pressure loss, ξ is the local resistance factor, Q is the flow rate when the oil flows through the bended places of pipeline.

3.5 TORTIONAL MOMENT ANALYSIS

The torsional moment of the shaft when the output displacements of the two actuators are different can be calculated as:

$$M_d = |\theta_1 - \theta_2| K_s \,, \quad (10)$$

where M_d is the torsional moment, $(\theta_1 - \theta_2)$ is the torsion angle of the shaft, K_s is the torsional rigidity.

According to the torsional moment calculated above, the counterforce and the deformation of piston rod can be presented as:

$$F = M_d / a = K_{s2} x_l \,, \quad (11)$$

where a is the effective arm, F is the counterforce on the piston rod.

4 Analysis of simulation results

The main simulation parameters are shown in Table 1.

TABLE 1 Main simulation parameters

Oil pressure	**Return pressure**	**Fixed stiffness**	**Joint stiffness**	**Piston quality**
21MPa	**0MPa**	**1e8N/m**	**1e8N/m**	**2kg**
External leakage coefficient	Internal leakage coefficient	Bypass orifice diameter	Oil density	Actuator quality
1e-18	**1.6e-13**	**0.5mm**	**850kg/m^3**	**12kg**
External radius of trapezoidal	Internal radius of trapezoidal	Piston diameter	Rod diameter	Pipe diameter
15mm	**7mm**	**0.1m**	**0.043m**	**10mm**

4.1 ASYMMETRY OF PIPELINE

The asymmetry of pipeline is an obvious factor which will cause the desynchrony of the two channels. To analyse the influence of this factor on force-fight, assume that the two valves have the same dead band and the zero offset is ignored. Set the external pipeline's length of valve 1 and valve 2 to 1.8m and 0.75m respectively. The simulation results of the fighting-force caused by the asymmetry of pipeline are presented in Figure 4 when the input displacement of joystick is ±10mm (step).

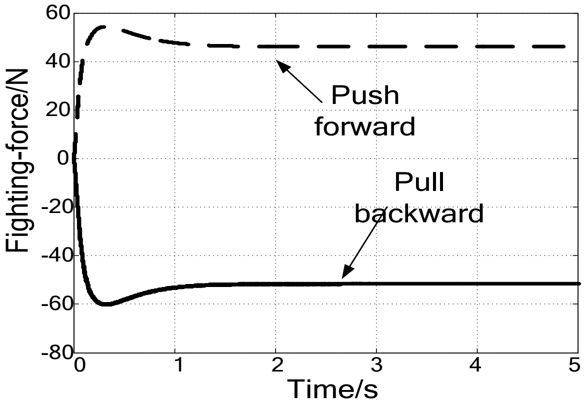

FIGURE 4 Fighting-force of asymmetric pipeline

Simulation results show that, when the difference of the pipeline's length is 1.05m, the fighting-force is very small. So the influence of the asymmetry of pipeline on force-fight can be neglected.

4.2 DIFFERENCE OF DEAD BAND

The overlap valve is widely used in practical applications, but the manufacture error and wear will both lead to the difference of the two valves' dead band inevitably. Without consideration of zero offset, set the difference of two valves' dead band to 0.01~0.04mm, and the dead band of valve 1 is 0.04mm which is smaller than valve 2's. The simulation results of fighting-force are presented in Figure 5.

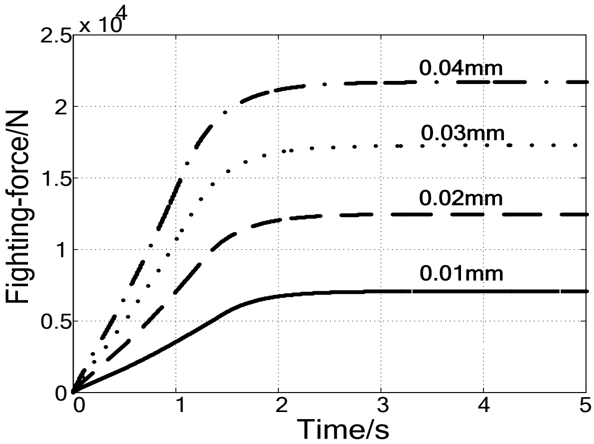

FIGURE 5 Valve 1's dead band is smaller

In Figure 6, valve 2's dead band is set to 0.04mm which is smaller than valve 1's and other conditions is the same as before.

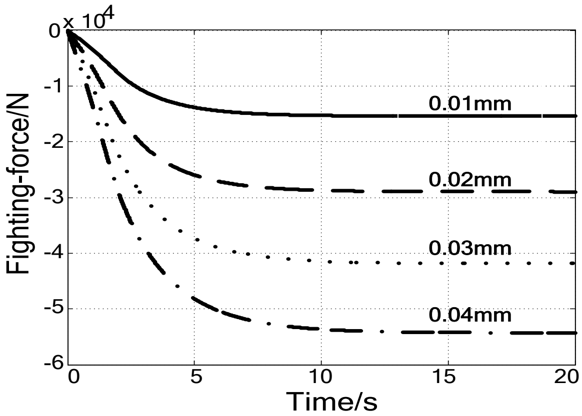

FIGURE 6 Valve 1's dead band is larger

List the data of fighting-force in the two cases above in Table 2.

TABLE 2 Fighting-force changes with the difference of valve's dead band

Difference of dead band/mm (valve 1 is smaller)	**0.01**	**0.02**	**0.03**	**0.04**
Fighting-force/N	8430	14800	20400	25600
Difference of dead band/mm (valve 1 is larger)	0.01	0.02	0.03	0.04
Fighting-force /N	15460	29030	41910	54350

As show in Table 2 when the dead band of valve 1 is smaller, for every increase in the difference of the two valves' dead band of 0.01mm the fighting-force increase around 5000N; when the dead band of valve 1 is larger for every increase in the difference of the two valves' dead band of 0.01mm the fighting-force increase around 12000N.

The fighting-force is obviously different in the two cases because the feedback channel is controlled by valve 1. In the former case, valve 1 is always open until both of the valves are closed so the feedback process is very quick; In the latter case after valve 1 is closed, rod 2 drags rod 1 to produce feedback signal until the two valves are closed so the feedback process is very slow that is why the fighting-force is very large .

4.3 SPEED OF DRIVING MOTOR

For the joystick is controlled by motor, the input displacement signal is impossible to achieve the given value immediately, so it is necessary to analysis the influence of the driving speed on system's force-fight.

The zero offset is ignored and the dead band of valve 1 and valve 2 is 0.04mm and 0.052mm respectively, the joystick is pushed forward by 10mm (step). The simulation results are presented in Figure 7 when the driving speed is set to 10mm/s, 20mm/s, 50mm/s and 100mm/s.

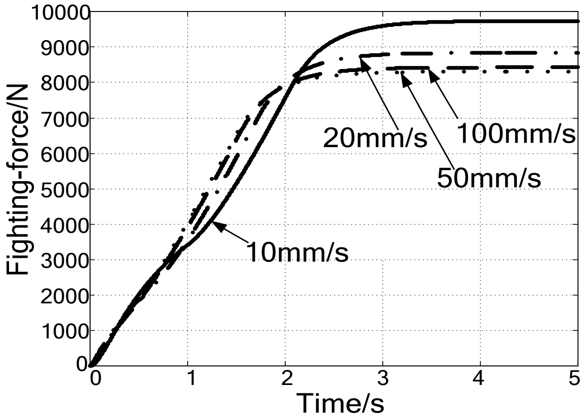

FIGURE 7 Fighting-force of different driving speed

According to the simulation results the fighting-force decrease with the increase of the driving speed but when the speed is more than 50mm/s, the fighting-force remain basically unchanged.

4.4 ADOPT BYPASS ORIFICE

When the parameters of valves and driving speed is restricted, adopting the bypass orifice to connect the two cavities of the actuator cylinder to reduce fighting-force.

4.4.1 Adopt fixed orifice

Adopt a fixed orifice whose diameter is 0.05mm and length is 8mm to connect the two cavities. When there is no aerodynamic load the dead band of the two valves is 0.04mm and 0.052mm respectively, the simulation results are presented in Figure 8 when the input displacement is 10mm (step).

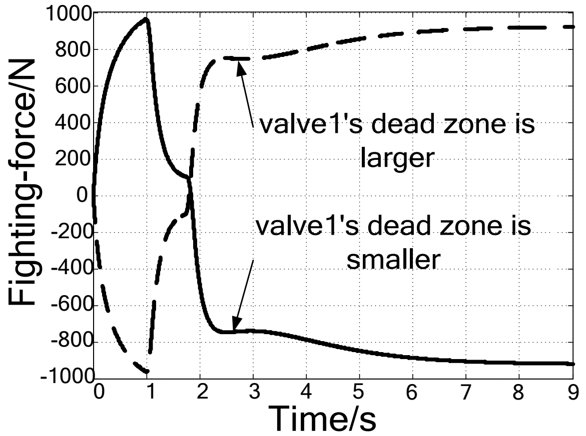

FIGURE 8 Fighting-force when adopt fixed orifice

Simulation results show that in the two cases the fighting-force are both very small, and the fighting-force in the two cases are basically the same, that is because the two valves are always open to supply the flow rate when the bypass orifice is adopted.

The influence of the diameter of the orifice is analyzed through simulation below. The valve 1's dead band is 0.04mm and the valve 2's dead band is 0.052mm, and the diameter of bypass orifice is set to 0.2mm~0.5mm. The simulation results are presented in Figure 9 when there is no aerodynamic load.

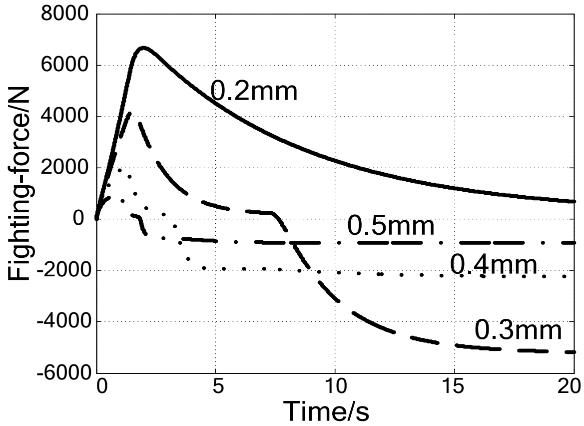

FIGURE 9 Different diameter of bypass orifice

The simulation results show that, the fighting-force decrease obviously with the increase of the diameter. The fighting-force reduce 2000N for every increase in the diameter of 0.1mm, and the stabilizing process is slow when the diameter is small.

4.4.2 Adopt variable orifice

To reduce the oil consumption, adopt the variable orifice, the area of the variable orifice can be obtained as:

$$f = \pi r^2 (1 - \frac{\Delta p}{p_i}), \tag{12}$$

where P_i is the threshold differential pressure.

With the increase of ΔP the area of the orifice will decrease, and when $\Delta P \geqq P_i$ the orifice closes. This design is to reduce ΔP of the two cavities during the initial procedure to reduce the fighting-force, and keep a certain differential pressure during the stabilizing process to guarantee the response speed of system.

The largest diameter of the orifice is 0.5mm, and its length is 8mm, the threshold differential pressure is 5MPa, the dead band of the two valves is 0.04mm and 0.052mm respectively. Simulation results of fighting-force are presented in Figure 10.

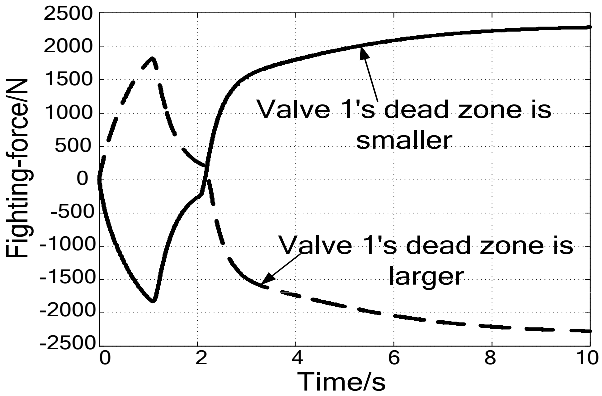

FIGURE 10 Adopt variable bypass orifice

Simulation results show that the fighting-force is around 2400N, which is a little bigger than adopting the fixed orifice, but is relatively small. For the area of the orifice is variable the wastage of hydraulic oil is reduced and the stabilizing process is accelerated.

5 Experimental verification

In the test, the input displacement signal is the sinusoidal waves of frequency 0.05Hz~0.9Hz and amplitude 5mm, the dead band of valve 1 and valve 2 is 0.04mm and 0.052mm respectively and there is no aerodynamic load. In the case of without bypass orifice, the test and simulation results are listed in Table 3.

TABLE 3 Simulation results contract with test results

Frequency/Hz	**0.05**	**0.1**	**0.2**	**0.3**	**0.4**
FF of simulation/KN	20.9	11.2	5.72	3.88	2.95
FF of test/KN	21.3	11.7	6.1	4.09	3.17
Frequency/Hz	0.5	0.6	0.7	0.8	0.9
FF of simulation/KN	2.38	2	1.73	1.52	1.36
FF of test/KN	2.52	2.23	1.97	1.78	1.54

Simulation and test results of adopting bypass orifice of 8mm diameter and 0.5mm length are listed in Table 4.

TABLE 4 Simulation results contract with test results when adopt bypass orifice

Frequency/Hz	**0.05**	**0.1**	**0.2**	**0.3**	**0.4**
FF of simulation/KN	1.51	1.35	1.01	0.1	0.97
FF of test/KN	1.83	1.62	1.13	1.08	1.35
Frequency/Hz	0.5	0.6	0.7	0.8	0.9
FF of simulation/KN	0.94	0.916	0.891	0.866	0.84
FF of test/KN	1.42	1.16	1.10	0.99	0.90

The data show that the simulation error remains below 8%, which means this model can be used as an accurate simulation platform to solve the force-fight problem of aileron. For the inconsistent of the clearance in mechanical transmission is ignored in the model, the simulation results are always smaller. Simulation and test results show that when the frequency of input signal is low the method of adopting the bypass orifice can reduce the fighting-force greatly, with the increase of the frequency the adopting of bypass-orifice has relatively small impact on force-fight. When the frequency reaches 1Hz the fighting-force reduce to 1000N without any measurement.

6 Conclusions

(1) The asymmetry of pipelines has little impact on the force-fight, so it is unnecessary to consider this factor in the pipeline layout;
(2) The difference of two valves dead band has great influence on force-fight, so it is important to reduce this difference. Set the dead band of the valve which control the feedback loop smaller is conducive to the decrease of system’s fighting-force;
(3) Fighting-force will be great if the driving speed is too small, so this speed is recommended to be more than 50mm/s;
(4) Adopting bypass orifice can reduce the fighting-force greatly and the fighting-force will decrease with the increase of the orifice’s diameter;
(5) Adopting the variable orifice can reduce the wastage of hydraulic oil at the same time of obtaining a small fighting-force.

Acknowledgments

I would like to extend my sincere gratitude to my tutor, for his instructive advice and useful suggestions on my paper. Special thanks should go to my friends who have put considerable time and effort into their comments on the draft. This work was financially supported by National Natural Science Foundation of China (61374032/2013).

References

[1] Wang Zhanlin, Qiu Lihua, Zhang Xiaosha, et al 1991 Research on the synchronous drive of the redundant channels for hydraulic actuator *Journal of Astronautics* **12**(2) 9-14
[2] Annaz F Y 2005 *Smart Materials and Structures* **14**(6) 1227-38
[3] Maré J-C 2007 Comparison of Hydraulically and Electrically Powered Actuators with reference to Aerospace Applications. *Hydraulics and Pneumatics Conference*
[4] Cochoy O, Hanke S, Carl U B 2007 *Aerospace Science and Technology* **11**(2) 194-201
[5] O’brien M 1998 *Aircraft Engineering and Aerospace Technology* **70**(5) 364-6
[6] van Den Bossche D The A380 flight control electrohydrostatic actuators achievements and lessons learnt. 25th international congress of the aeronautical sciences, Hamburg, Germany, 3–8 September 2006 *session 7.4.1* 1–8
[7] Straub H H, Creswell R 1991 *Aerospace Technology Conference and Exposition* Long Beach: CAUnited States 31-40
[8] Wang Zhengjie, Guo Shijun, Li Wei 2008 *WSEAS Transactions on Systems and Control* **3**(10) 869-78
[9] Nagai Kiyoshi, Dake Yuichiro, Shiigi Yasuto, et al 2010 Design of redundant drive joints with double actuation using springs in the second actuator to avoid excessive active torques *2010 IEEE International Conference on Robotics and Automation (ICRA)* Anchorage, AK 805-12
[10] Zhang J, Gao F, Yu H, et al 2011 *Journal of Mechanical Engineering Science* **225**(12) 3031-44
[11] Patra K C 2011 *Engineering fluid mechanics and hydraulic machines* Oxford UK: Alpha Science International
[12] Karam W, Mare J-C 2009 *Aerospace Eng Aircraft Technol* **81**(4) 288–98
[13] Attar B 2008 *Realistic modelling in extreme conditions of electro-hydraulic servovalve used for aerospace guidance and navigation* France: PhD Thesis, INSA Toulouse
[14] Fu Y L, Liu H S, Pang Y, et al 2010 Force fighting research of dual redundant hydraulic actuation system. 2010 *international conference on intelligent system design and engineering application, Beijing, China, 13–14 October 2010* China: Beihang University 762–6
[15] Jacazio G, Gastaldi L 2008 Equalization techniques for dual redundant electro hydraulic servo actuators for flight control systems. *Bath/ASME Symposium on Fluid Power and Motion Control (FPMC 2008)* Bath, 2008 543-57
[16] Qi H T, Mare J-C, Fu Y L 2009 Force equalization in hybrid actuation systems *7th international conference on fluid power transmission and control, Hangzhou,China, 7–10 Apr 2009* China: Zhejiang University 342–7

[17] Cheng Hui, Yiu Yiu-Kuen, Li Zhang 2003 *IEEE/ASME Transactions on Mechatronics* **8**(4) 483-91

[18] Mare J-C, Moulaire P 2001 The decoupling of position controlled electrohydraulic actuators mounted in tandem or in serie *Seventh Scandinavian International Conference on Fluid Power* Linkoping 93-108

[19] Steffen T, Davies J, Dixon R, Goodall R M 2007 Using a Series of Moving Coils as a High Redundancy Actuator *Preprint of the IFAC Conference for Advanced Intelligent Mechatronics* (AIM) Zurich

[20] Ifrim A M 2013 *Electrotehnica, Electronica, Automatica* **61**(2) 79-84

Authors

Ying Zhang, born on November 2, 1984, Hubei, China

Current position, grades: PhD studies in Detection Technology and Automatic Equipment
University study: M.Sc. in Mechanical Engineering from Northwestern Polytechnical University.
Research interests: servo control and design of hydraulic system

Zhaohui Yuan, born in March, 1964, Anhui, China

Current position, grades: full Professor in School of automation, Northwestern Polytechnical University
University study: M.Sc. in Transmission and Control of fluid and PhD in Detection Technology and Automatic Equipment
Research interests: different aspects of servo control systems